Science Advances
AAAS

advances.sciencemag.org/cgi/content/full/5/9/eaaw3350/DC1

Supplementary Materials for

Aluminum-26 chronology of dust coagulation and early solar system evolution

M.-C. Liu*, J. Han, A. J. Brearley, A. T. Hertwig

*Corresponding author. Email: mcliu@ucla.edu

Published 11 September 2019, *Sci. Adv.* **5**, eaaw3350 (2019)
DOI: 10.1126/sciadv.aaw3350

This PDF file includes:

Supplementary Materials and Methods

Sample description

Hibonite crystals: 019, 176, and 181

019: This inclusion consists only of hibonite crystals. They are closely distributed in the matrix and may be fragments of a larger inclusion.
176: This inclusion is a hibonite crystal with minor perovskite.
181: This CAI is an elongated hibonite crystal containing subrounded to elongated perovskite grains.

Corundum-bearing, hibonite-rich inclusions: 030 and 086.

030: This inclusion is dominated by hibonite laths surrounded by spinel. Minor corundum occurs in hibonite. Perovskite occurs in hibonite and, with much finer size, in spinel.
086: This inclusion consists of hibonite and corundum. Al-Ti-rich unknown oxide (possibly perovskite due to mixed x-ray signal with corundum?) was identified.

Hibonite-bearing, spinel-rich inclusions: 021, 073, 117, 119, 147, 148, 164, 222, and 230

021: This inclusion consists predominantly of spinel, accompanied by hibonite laths and fine-grained perovskite grains.
073: This inclusion has randomly oriented hibonite laths embedded in spinel, with minor perovskite.
074: This CAI appears to have a concentric structure consisting of a hibonite-rich core surrounded by spinel. The hibonite-rich core is the aggregates of randomly oriented hibonite laths with subrounded perovskite grains that are partially surrounded by spinel.
095: In this CAI, hibonite is attached to spinel.
117: Hibonite laths are partially embedded in spinel, finally partially rimmed by diopside. Minor perovskite is present in hibonite and spinel.
119: This inclusion appears to have three nodules consisting of hibonite laths embedded in spinel, finally rimmed by diopside. A perovskite grain occurs only in spinel.
147: This inclusion is a single nodule consisting of hibonite embedded in spinel, finally completely rimmed by diopside.
148: Hibonite laths are partially to completely embedded in spinel, finally rimmed by diopside.
155: Two different orientations of hibonite laths are attached to spinel.
164: This CAI consists of randomly-oriented hibonite laths embedded in spinel, finally partially rimmed by diopside.
222: This inclusion contains hibonite and spinel, partially surrounded by diopside.
230: This CAI has randomly-oriented hibonite laths embedded in spinel.
230SW: This CAI has randomly-oriented hibonite laths embedded in spinel.

Hibonite-free, spinel-rich inclusions: 070, 165, 212, and 229

070: This CAI consists of elongated spinel cores surrounded by intergrowth layers of spinel and Al-Ti-rich pyroxene, finally rimmed by diopside. Thin layers of forsteritic olivine often occur on the exterior of diopside rim. Minor perovskite is present in spinel.
165: In this CAI, spinel is partially surrounded by intergrowth layers of spinel and Al-Ti-rich pyroxene, followed by diopside, olivine, and finally diopside.

212: This inclusion is a single nodule consisting of a spinel core surrounded by an intergrowth layer of spinel and Al-Ti-rich pyroxene, finally completely rimmed by diopside. Minor forsteritic olivine occurs on the exterior of diopside rim. Minor perovskite is present in spinel.
229: This inclusion consists of spinel cores separated by intergrowth layers of spinel and Al-Ti-rich pyroxene, finally rimmed by diopside. Thin layers of forsteritic olivine with minor Fe,Ni-metal often occur on the exterior of diopside rim. Perovskite and rare melilite occur in spinel.

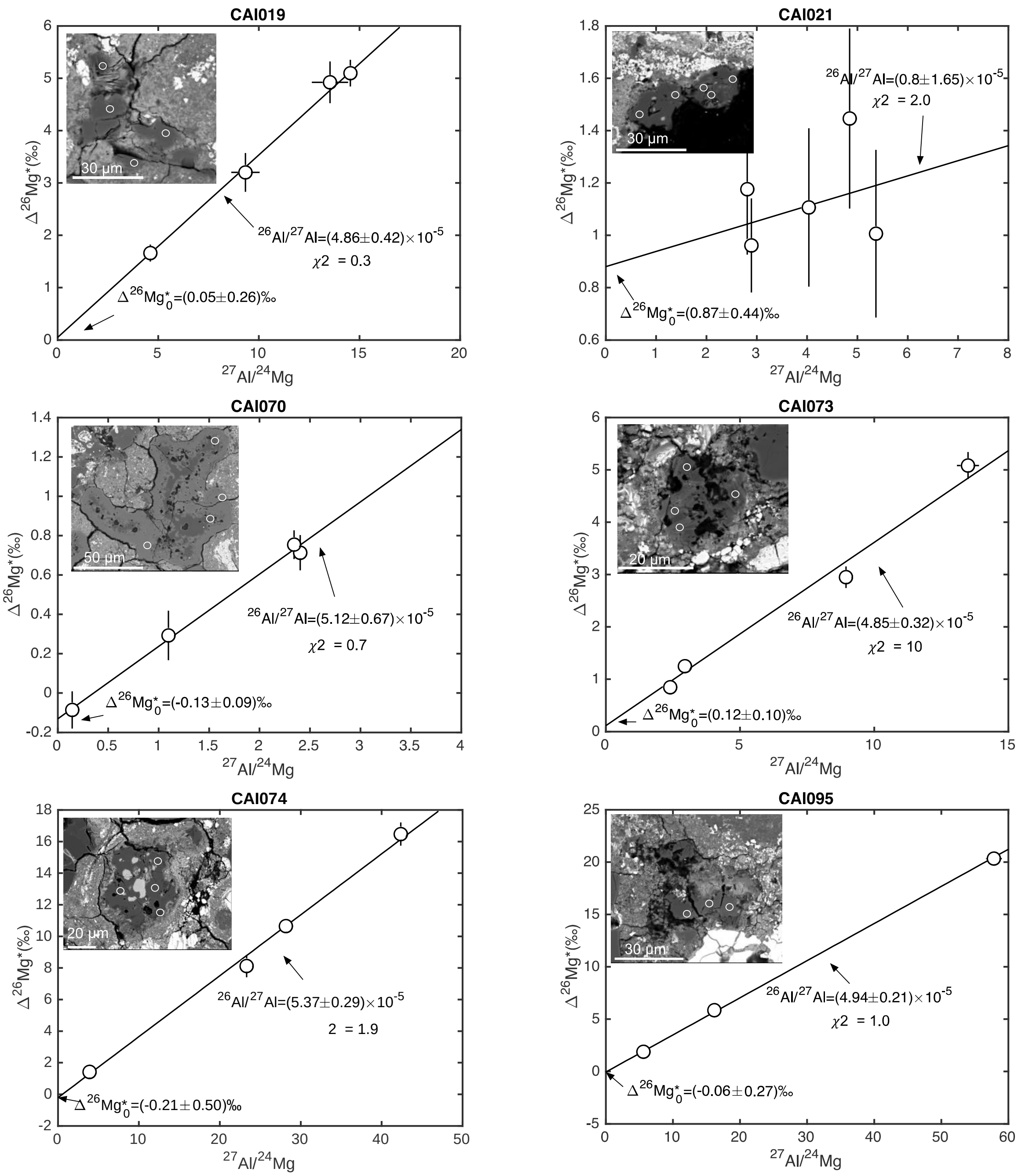
CAI019
$^{26}Al/^{27}Al=(4.86\pm0.42)\times10^{-5}$
$\chi2$ = 0.3
$\Delta^{26}Mg^*_0=(0.05\pm0.26)$‰
30 μm
$\Delta^{26}Mg^*$(‰)
$^{27}Al/^{24}Mg$
CAI021
$^{26}Al/^{27}Al=(0.8\pm1.65)\times10^{-5}$
$\chi2$ = 2.0
$\Delta^{26}Mg^*_0=(0.87\pm0.44)$‰
30 μm
$\Delta^{26}Mg^*$(‰)
$^{27}Al/^{24}Mg$
CAI070
$^{26}Al/^{27}Al=(5.12\pm0.67)\times10^{-5}$
$\chi2$ = 0.7
$\Delta^{26}Mg^*_0=(-0.13\pm0.09)$‰
50 μm
$\Delta^{26}Mg^*$(‰)
$^{27}Al/^{24}Mg$
CAI073
$^{26}Al/^{27}Al=(4.85\pm0.32)\times10^{-5}$
$\chi2$ = 10
$\Delta^{26}Mg^*_0=(0.12\pm0.10)$‰
20 μm
$\Delta^{26}Mg^*$(‰)
$^{27}Al/^{24}Mg$
CAI074
$^{26}Al/^{27}Al=(5.37\pm0.29)\times10^{-5}$
2 = 1.9
$\Delta^{26}Mg^*_0=(-0.21\pm0.50)$‰
20 μm
$\Delta^{26}Mg^*$(‰)
$^{27}Al/^{24}Mg$
CAI095
$^{26}Al/^{27}Al=(4.94\pm0.21)\times10^{-5}$
$\chi2$ = 1.0
$\Delta^{26}Mg^*_0=(-0.06\pm0.27)$‰
30 μm
$\Delta^{26}Mg^*$(‰)
$^{27}Al/^{24}Mg$

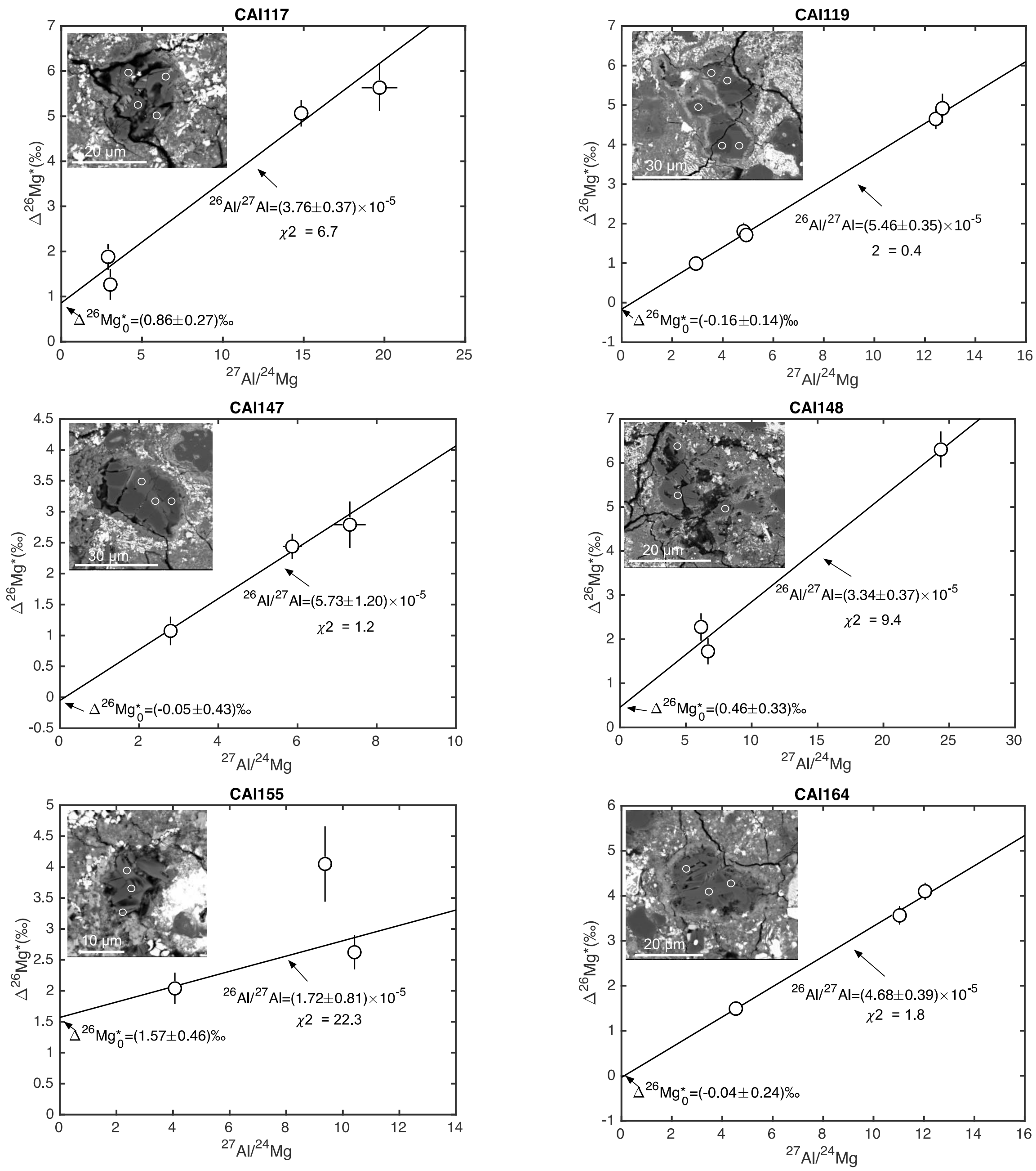

CAI117
20 μm
^{26}Al/^{27}Al=(3.76±0.37)×10^{-5}
χ2 = 6.7
Δ^{26}Mg*$_0$=(0.86±0.27)‰
Δ^{26}Mg*(‰)
^{27}Al/^{24}Mg
CAI119
30 μm
^{26}Al/^{27}Al=(5.46±0.35)×10^{-5}
2 = 0.4
Δ^{26}Mg*$_0$=(-0.16±0.14)‰
Δ^{26}Mg*(‰)
^{27}Al/^{24}Mg
CAI147
30 μm
^{26}Al/^{27}Al=(5.73±1.20)×10^{-5}
χ2 = 1.2
Δ^{26}Mg*$_0$=(-0.05±0.43)‰
Δ^{26}Mg*(‰)
^{27}Al/^{24}Mg
CAI148
20 μm
^{26}Al/^{27}Al=(3.34±0.37)×10^{-5}
χ2 = 9.4
Δ^{26}Mg*$_0$=(0.46±0.33)‰
Δ^{26}Mg*(‰)
^{27}Al/^{24}Mg
CAI155
10 μm
^{26}Al/^{27}Al=(1.72±0.81)×10^{-5}
χ2 = 22.3
Δ^{26}Mg*$_0$=(1.57±0.46)‰
Δ^{26}Mg*(‰)
^{27}Al/^{24}Mg
CAI164
20 μm
^{26}Al/^{27}Al=(4.68±0.39)×10^{-5}
χ2 = 1.8
Δ^{26}Mg*$_0$=(-0.04±0.24)‰
Δ^{26}Mg*(‰)
^{27}Al/^{24}Mg

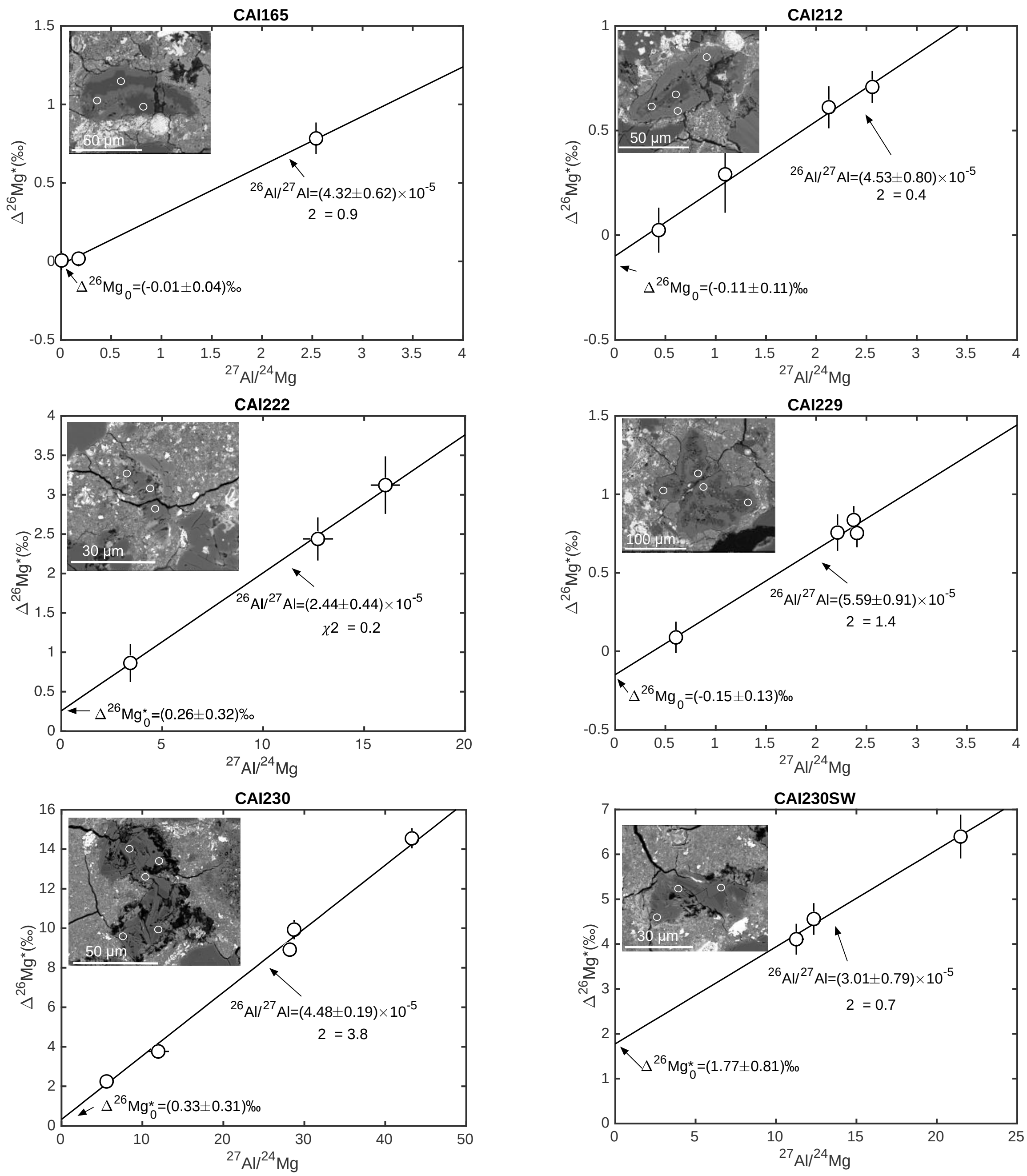

Fig. S1. Individual internal ^{26}Al isochrons obtained in 18 ^{26}Al-bearing inclusions. Errors are 2σ.

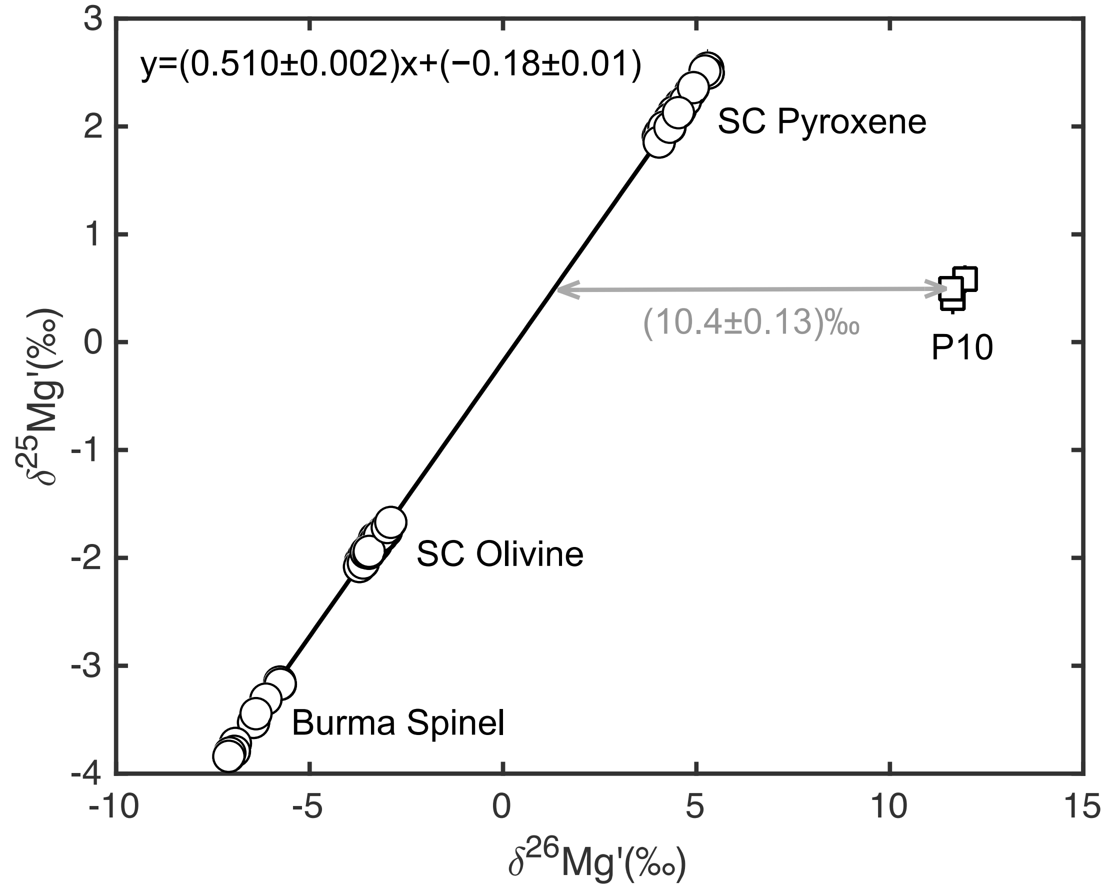

Fig. S2. Example of IMF characterized in one analysis session. Measurements on three magnesium-rich standards yielded a slope of 0.510 (±0.002) in δ^{25}Mg'−δ^{26}Mg' space (see above for the definition of δ^{i}Mg'). An in-house P10 glass (Δ^{26}Mg* = 10.3‰) was used as a secondary standard to check the measurement accuracy.

Table S1. Magnesium isotopic compositions of 22 inclusions analyzed in this study. δ^{25}Mg values have been corrected for instrumental mass fractionation by using the corresponding standards. h: hibonite; s: spinel; d: Al-Ti-rich diopside; f: forsterite.

Sample/spot	Ip (nA)	^{24}Mg (cps)	δ^{25}Mg (‰, ±2σ)	^{27}Al/^{24}Mg (±2σ)	Δ^{26}Mg* (‰, ±2σ)
CAI 019					
h1	8	3.24×10^{7}	−1.92±0.36	14.55±0.27	5.10±0.26
h2	8	4.90×10^{7}	−2.20±0.37	13.53±0.90	4.92±0.40
h3	8	3.92×10^{7}	−1.94±0.37	9.33±0.71	3.20±0.37
h4	8	1.17×10^{8}	−2.35±0.34	4.61±0.09	1.66±0.16
CAI 021					
h1		1.83×10^{7}	−3.03±0.37	4.85±0.03	1.45±0.34
h2	1	2.56×10^{7}	−3.75±0.35	4.03±0.03	1.11±0.30
s1	1	2.96×10^{7}	−4.54±0.36	2.81±0.02	1.18±0.25
h3	1	1.91×10^{7}	−2.89±0.38	5.37±0.06	1.01±0.32
s2	1	3.13×10^{7}	−2.57±0.45	2.89±0.02	0.96±0.18
CAI 030					
h1	5	2.00×10^{7}	−8.02±0.39	36.55±0.35	−0.23±0.35
h2	5	2.74×10^{7}	−4.44±0.37	20.51±0.60	−0.12±0.31
h3	5	1.20×10^{7}	−2.20±0.43	43.45±0.58	0.29±0.45
CAI 070					
s1	8	2.21×10^{8}	0.64±0.21	2.40±0.02	0.71±0.09
s2	8	2.28×10^{8}	0.67±0.20	2.34±0.02	0.75±0.07
d1	8	1.38×10^{8}	−0.52±0.28	1.10±0.05	0.29±0.13
d2	8	1.64×10^{8}	−0.30±0.27	0.14±0.01	−0.09±0.09
CAI 073					
h1	5	5.08×10^{7}	−0.08±0.36	13.49±0.41	5.08±0.26
h2	5	7.44×10^{7}	−4.16±0.36	8.95±0.23	2.95±0.21
s1	5	1.13×10^{8}	−1.64±0.34	2.95±0.03	1.25±0.08
s2	5	1.42×10^{8}	2.89±0.34	2.40±0.03	0.85±0.10
CAI 074					
h1	3	1.12×10^{7}	−2.73±0.58	28.16±0.44	10.64±0.42
h2	5	7.63×10^{6}	−2.22±0.49	42.36±0.61	16.47±0.74
h3	3	1.01×10^{7}	−2.66±0.51	23.31±0.85	8.12±0.71
h4 (overlapping spinel)	1	1.56×10^{7}	−3.98±0.51	3.90±0.15	1.42±0.46
CAI 086					
h1	5	9.81×10^{6}	−1.67±0.50	32.12±1.34	−0.40±0.49

h2	3	9.03×10^{6}	−1.12±0.48	20.02±0.33	−0.85±0.43
CAI 095					
h1	5	3.10×10^{7}	−2.42±0.36	16.17±0.61	5.86±0.35
h2	5	1.17×10^{7}	−2.76±0.42	57.84±1.18	20.34±0.64
h3	5	8.40×10^{7}	−2.57±0.36	5.60±0.40	1.88±0.20
CAI 117					
h1	3	2.00×10^{7}	−1.51±0.47	14.85±0.37	5.07±0.29
h2	3	1.29×10^{7}	−0.56±0.49	19.70±1.11	5.63±0.52
s1	1	1.78×10^{7}	−1.29±0.46	2.90±0.04	1.88±0.29
s2 (overlapping hibonite)	1	1.42×10^{7}	0.34±0.49	3.04±0.05	1.27±0.34
CAI 119					
h1	8	6.31×10^{7}	−3.76±0.34	12.43±0.22	4.65±0.26
s1	8	2.09×10^{8}	−4.29±0.33	2.94±0.06	0.99±0.10
h2	8	6.55×10^{7}	−6.14±0.34	4.83±0.24	1.81±0.22
h3	8	1.28×10^{8}	−5.18±0.33	4.93±0.20	1.71±0.17
h4	8	3.17×10^{7}	−5.81±0.35	12.69±0.17	4.92±0.37
CAI 147					
h1	3	2.92×10^{7}	−1.23±0.46	7.32±0.40	2.79±0.38
s1	1	2.73×10^{7}	−3.58±0.46	2.79±0.04	1.07±0.23
h2	3	3.36×10^{7}	−1.35±0.47	5.87±0.24	2.44±0.21
CAI 148					
h1	5	1.54×10^{7}	−0.06±0.48	24.36±0.47	6.30±0.41
h2	3	2.96×10^{7}	−1.28±0.47	6.15±0.12	2.28±0.31
h3	3	3.06×10^{7}	−1.85±0.47	6.68±0.14	1.73±0.30
CAI 155					
h1	3	2.35×10^{7}	2.84±0.46	10.41±0.19	2.62±0.28
h2 (overlapping spinel)	1	1.83×10^{7}	3.56±0.46	4.07±0.06	2.04±0.25
h3	1	6.89×10^{6}	2.10±0.54	9.37±0.25	4.05±0.61
CAI 164					
h1 (overlapping spinel)	5	1.19×10^{8}	−3.49±0.36	4.54±0.03	1.49±0.13
h2	5	4.95×10^{7}	−3.58±0.35	12.04±0.26	4.10±0.19
h3	5	4.93×10^{7}	−1.34±0.35	11.04±0.15	3.56±0.21
CAI 165					
s1	8	2.29×10^{8}	−0.08±0.20	2.54±0.01	0.78±0.10
f1	8	4.44×10^{8}	−0.10±0.15	$(8.65\pm0.73)\times10^{-4}$	0.01±0.06

d1	8	3.47×10^{8}	1.25±0.26	0.17±0.01	0.02±0.25
CAI 176					
h1	8	2.18×10^{7}	−9.31±0.40	4.20±0.13	−0.41±0.48
h2	8	2.79×10^{7}	−9.30±0.39	29.13±0.30	−0.71±0.39
h3	8	2.14×10^{7}	−8.12±0.43	8.52±0.21	−0.49±0.45
CAI 181					
h1	8	8.65×10^{6}	−8.90±0.55	48.92±0.61	1.27±1.00
h2	8	1.10×10^{7}	−8.05±0.48	33.28±0.46	−2.75±0.93
h3	8	2.15×10^{7}	−8.29±0.39	23.31±0.25	−0.57±0.48
CAI 212					
s1	8	2.48×10^{8}	−0.33±0.20	2.56±0.02	0.71±0.08
d1	8	7.71×10^{7}	−0.05±0.28	1.09±0.01	0.29±0.18
d2	8	1.66×10^{8}	3.21±0.27	0.43±0.03	0.02±0.11
s2 (overlapping diopside)	8	1.95×10^{8}	0.94±0.20	2.12±0.02	0.61±0.10
CAI 222					
h1	3	2.08×10^{7}	−2.15±0.52	16.05±0.73	3.12±0.36
h2	3	3.17×10^{7}	−5.19±0.48	12.71±0.75	2.44±0.27
h3 (overlapping spinel)	1	2.05×10^{7}	−2.82±0.46	3.42±0.05	0.86±0.24
CAI 229					
s1	8	2.02×10^{8}	1.13±0.20	2.41±0.01	0.75±0.09
d1	8	1.49×10^{8}	0.43±0.27	0.60±0.02	0.09±0.10
s2	8	2.14×10^{8}	1.27±0.20	2.37±0.01	0.84±0.09
s3	8	1.98×10^{8}	1.49±0.21	2.21±0.01	0.76±0.12
CAI 230					
h1	5	9.60×10^{6}	0.56±0.52	43.29±0.61	14.55±0.51
h2	3	3.80×10^{7}	−3.94±0.45	5.57±0.13	2.25±0.28
h3	5	1.52×10^{7}	0.27±0.51	28.20±0.55	8.92±0.37
h4	5	3.99×10^{7}	−4.08±0.46	11.95±1.33	3.77±0.38
h5	5	1.21×10^{7}	0.34±0.48	28.74±0.54	9.93±0.49
CAI 230SW					
h1	3	1.09×10^{7}	−0.30±0.51	21.48±0.31	6.40±0.49
h2	3	2.29×10^{7}	−2.74±0.46	11.26±0.49	4.11±0.34
h3	5	1.78×10^{7}	0.17±0.49	12.35±0.20	4.56±0.35

Table S2. Relative sensitivity factors determined on standards with known $^{27}Al/^{24}Mg$ in three analysis sessions. Errors are 2 standard deviations.

Standard	Session 1	Session 2	Session 3
P0 glass	1.17±0.04	1.21±0.04	1.19±0.04
Burma spinel	1.29±0.01	1.37±0.02	1.31±0.02
Madagascar hibonite	1.30±0.15	1.36±0.11	1.34±0.20